Molecular Crystals and Liquid Crystals
Publication details, including instructions for authors and subscription information:
http://www.tandfonline.com/loi/gmcl20

Optical Multimode Interference Router in Sol-gel Waveguide with a Liquid Crystal Cladding

Luigi Sirleto [a], Giuseppe Coppola [b] & Giovanni Breglio [b]

[a] Research Insitute for Electromagnetism and Electronic components-CNR, I.R.E.C.E., Via Diocleziano 328, Naples, 80124, Italy

[b] Department of Electronic Engineering and Telecommunications, University 'Federico II', Via Claudio 21, Naples, 80125, Italy

Version of record first published: 18 Oct 2010

To cite this article: Luigi Sirleto, Giuseppe Coppola & Giovanni Breglio (2002): Optical Multimode Interference Router in Sol-gel Waveguide with a Liquid Crystal Cladding, Molecular Crystals and Liquid Crystals, 375:1, 107-119

To link to this article: http://dx.doi.org/10.1080/10587250210590

Mol. Cryst. Liq. Cryst., Vol. 375, pp. 107-119

1058-725X/02 $12.00 + .00

Optical Multimode Interference Router in Sol-gel Waveguide with a Liquid Crystal Cladding

LUIGI SIRLETO, GIUSEPPE COPPOLA[a] and GIOVANNI BREGLIO[a]

I.R.E.C.E.-Research Insitute for Electromagnetism and Electronic components-CNR, Via Diocleziano 328, 80124 Naples, Italy and [a]*Department of Electronic Engineering and Telecommunications, University 'Federico II', Via Claudio 21, 80125 Naples, Italy*

The self-imaging principle has been applied in the design of a novel configuration for an electro-optical router, working at the wavelength of 1.55 micron. The device is composed by: a single mode input optical channel waveguide; a bimodal active region, having a liquid crystal as over-layer; an output Y branch, to separate the two output channels. The active region is designed to allow a π shift between the two modes that it supports, by means of electro-optic effect of smectic A*, in order to steer light from one output channel to the other one.

In this paper, for the first time, the performances of an electro-optical router, based on the multimode interference effects together with the electro-optic effect of smectic A* liquid crystal, are theoretically and numerically discussed.

Keywords: integrated optics; electro-optic devices; routing devices; paraelectric liquid crystals; self imaging principle

INTRODUCTION

Today's evolving telecommunication networks are increasingly focusing on flexibility and reconfigurability, which requires enhanced functionality of photonic integrated circuits (PIC's) for optical

communications. In addition, modern wavelength demultiplexing (WDM) systems will require signal routing and coupling devices to have small dimensions and improved fabrication tolerances in order to reduce process costs and contribute to large-scale PIC production.

Integrated optical devices based on multimode interference (MMI) effects fulfill all of the above requirements. Their excellent properties and easy of fabrication have led to their rapid incorporation in more complex PIC's such as: Mach-Zender switches [1]; modulator [2]; coherent receivers [3]; and ring lasers [4].

On the other hand, in recent years several authors suggested and demonstrated the possibility of using Liquid Crystals (LC's) materials to control the light propagation in optical guiding devices, as planar waveguides or cylindrical fibers[5-11]. The main features of LC's, such as: the high sensitivity of their optical response to an applied electrical field or an optical field, their ability to be micro manipulated, their low cost and the possibility for integration with silicon circuit technology; make them particularly attractive in designing integrated optics components.

Routing devices do not require very high switching time performances but have to guarantee low optical insertion loss and quite good performances in term of crosstalk. It is worth to note that routing devices, based on different materials and physical effects, have already been presented in literature [12-15]. However, at least in our knowledge, routing devices based on liquid crystals have never been analyzed. So, in this paper, a novel configuration for an integrated router, based on the mode-mixing principle together with the electro-optic effect of a *smectic A** liquid crystal [16-22] and working at the wavelength of 1.55 micron, is theoretically discussed and numerically analyzed, for the first time. Exhaustive details about the design together with the description of the optical behavior of device will be given. Numerical simulations have shown that the router exhibits satisfactory performances.

THE SELF-IMAGING PRINCIPLE

The principle can be stated as follows: *Self-imaging is a property of multimode waveguide by which an input field profile is reproduced in single or multiple images at periodic intervals along the propagation direction of the guide* [23-27].

The central structure of an MMI device is a waveguide designed to support a large number of modes (typically 2). In order to launch light into and recover light from that multimode waveguide, a number of access (usually single-mode) waveguides are placed at its beginning and at its end. Such devices are generally referred to as NxM MMI couplers, where N and M are the number of input and output waveguides respectively.

Self-imaging may exist in three-dimensional multimode structure. However for step-index waveguide, which are, in general, single-mode in the transverse direction, it is justified to assume that the modes have the same transverse behavior everywhere in the waveguide. So the problem can thus be analyzed using a two-dimensional (lateral y axis and longitudinal z axis) structure without losing generality. The analysis hereafter is based on such 2-D representation of the multimode waveguide, which can be obtained from the actual 3-D physical multimode waveguide by several techniques such as the effective index method.

The propagation constants $\beta_{0\nu}$ of the modes, supported by a multimode waveguide (MMI section) with slab effective index of refraction N and width W, show a nearly quadratic dependence with the lateral mode number ν:

$$\hat{a}_{0i} \approx k_0 N - \frac{\delta(i+1)^2}{3L_\delta} \tag{1}$$

which follows from $k_y^2 + k_z^2 = k_0^2 N^2$ with $k_z = \hat{a}_{0i}$, $k_y \approx \frac{(i+1)\delta}{W}$, $k_0 = \frac{2\pi}{\lambda_0}$, the fact that $\hat{a}_{0i}$ is close to $k_0 N$ and from the definition of beat length $L_\pi = \frac{\pi}{\beta_{00} - \beta_{01}}$ [25,26].

The total lateral profile $h_x(y,z)$ at any z position in the MMI section can be written as a linear combination of the fields $h_{x,\nu}(y)$ of the M guided modes:

$$h_x(y,z) = \sum_{i=0}^{M-1} c_i h_{x,i}(y) \exp(-j\hat{a}_{0i} z) \tag{2}$$

where the coefficients c_ν determine the relative contribution of each mode. In particular, the total lateral field profile at the entrance (z=0) of the MMI section is:

$$h_x(y,0) = \sum_{\nu=0}^{M-1} c_\nu h_{x,\nu}(y) \tag{3}$$

which reflects the decomposition of the input field profile into all guided modes.

Using the propagation constants given by (1), the total lateral field profile at the end ($z = L_{MMI}$) of the MMI section can be found from

$$h_x(y,L_{MMI}) = \exp(-jk_0 N\ L_{MMI}) \sum_{i=0}^{M-1} c_i h_{x,i}(y) \exp\left(j\frac{\delta(i+1)^2 L_{MMI}}{3L_\delta} \right) \tag{4}$$

Inspection of the phase factor leads to the results (5) where q is an integer number and the overall phase factor $\exp(-jk_0 N L_{MMI})$ has been dropped.

$$h_x(y,L_{MMI}) = \begin{cases} \sum_{i=0}^{M-1} c_i h_{x,i}(y) = h_x(y,0) & L_{MMI} = (2q)3L_\delta \\ \sum_{i=0}^{M-1} (-1)^{i+1} c_i h_{x,i}(y) = -h_x(-y,0) & for\ L_{MMI} = (2q+1)3L_\delta \\ \frac{j(-1)^q + 1}{2} h_x(y,0) + \frac{j(-1)^q - 1}{2} h_x(-y,0) & L_{MMI} = \left(q + \frac{1}{2}\right)3L_\delta \end{cases} \tag{5}$$

The even and odd symmetry of the modes can be used to rewrite the previous results in terms of the total lateral field profile at the input. These results show that:

when $L_{MMI} = (2q)3L_\pi$ the field at the entrance is reproduced at the end of the MMI section (self-imaging effect), and the router is in the *bar state*;

when $L_{MMI} = (2q+1)3L_\pi$ the field at the end of the MMI section is an x-z plane mirror image of the field at the entrance, and the router is in the *cross state*;

when $L_{MMI}=\left(q+\frac{1}{2}\right)\beta L_{\pi}$ the field at the end of the MMI section is a linear combination of the original field at the entrance and its x-z plane mirror image with a relative phase of $\pi/2$. So a two-fold image is obtained.

STRUCTURE, WORKING PRINCIPLE OF DEVICE AND NUMERICAL REULTS

The router is composed by: a single mode input optical channel (rib) waveguide; a bimodal active region, having a liquid crystal as over-layer; an output Y branch, to separate the two output channels. In figure 1 the structure of our router is reported.

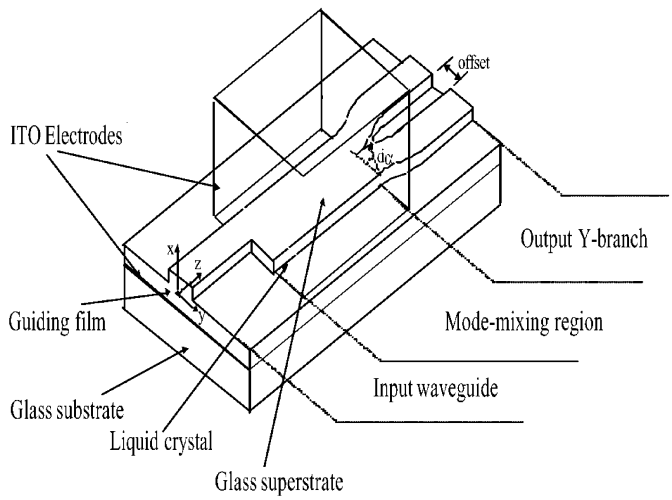

FIGURE 1 Schematic top view of the device.

The device may be built in silica-titania glass, by using a sol-gel deposition, on a glass substrate covered with an indium tin oxide (ITO) layer. The refractive index of the glass substrate is n_{sub}=1.516. The thickness of the ITO layer and its refractive index are: t_{ITO}=20 nm; n_{ITO}=1.9. The thickness of the ITO layer has been chosen in order to have negligible effects on the modal behavior [6,8]. The guiding film, having the refractive index: n_{film} = 1.670 at the wavelength λ=1.55 μm, may be built by sol-gel technique [28, 29].

In order to obtain the single mode input waveguide, a 3 μm wide and 1.2 μm etched rib waveguide may be built in a planar waveguide, having the thickness: t_g=3 μm. Using SELENE β0], for the calculation of the two-dimensional field profile in cross-section of the waveguide, a clear single mode behavior has been obtained. In the active region, a good confinement of both the fundamental mode (quasi TE_{00}) and the first higher mode (quasi TE_{01}) has to be guaranteed. On this account the width of the waveguide is doubled, thus obtaining a 6 μm x 3 μm rib waveguide. On the surface of the active region a thick layer of smetic A* liquid crystal (thickness > 5 μm) is placed. This latter is covered by a glass substrate, coated with ITO layer (see fig. 1). The two ITO layers constitute the electrodes to apply the electric field.

In chiral orthogonal smectic A (A^*) the optic axis lies in the direction of the smectic layer normal in the field-free state and, by applying an electric field *E*, the optic axis is forced to tilt out of this state by an angle $\theta(E)$ in a plane perpendicular to the field itself (*electroclinic effect*) [17-21]. Achievable tilt values are about 10 degrees and in about half of this range θ can be considered linear in the field. The deflection of the optic axis occurs in the opposite direction when we reverse the sign of the field. The most striking properties of the electroclinic effect are: its linearity versus the applied field; its very fast response time (sub-microsecond range), which is independent of the applied field. These appealing features of electroclinic effect are counterbalanced by strong temperature dependence. In order to obtain the best performance of devices based on this effect, a constant temperature must be imposed. This limitation can be easily overcome utilizing, for example, thermoelectric module based on Peltier effect.

Finally, the output Y-branch is realized by two S-bend waveguides, which are able to select one of the two output states of the active region. Both the waveguides of the branch are designed to sustain only the fundamental mode. Thus, these S-bend waveguides are 3 μm x 3 μm rib waveguides with a lateral etching of 1.2 μm, a radius of about 10 cm, $d\alpha$=0.3° and an offset of 20 μm (see fig. 1).

Working principle of device

How we can see from figure 1, the input waveguide is asymmetrically coupled to the active region. In this way, the fundamental (the quasi TE_{00}) mode coming from the input waveguide can excite both the fundamental mode and the first higher order mode in the active region, namely the quasi TE_{00} and TE_{01} modes, respectively. These two modes spatially interfere upon propagation in the active region, leading to a localized output power emerging on one of the two output sides. The length of the active region is designed to ensure that an additional π phase shift, between the two propagating modes in the active region, allows steering the light on the other side of the output.

The desired phase shift is reached by means the molecular reorientation of liquid crystals over-layer, induced by an electrical field. The change in the refractive index of the liquid crystal implies a change of the propagating characteristics (effective refractive indices) both of the fundamental mode and of first higher mode traveling in the active region. So the light can be steer between the two output sides of the Y-branch, simply switching the sign of electrical field applied on the liquid crystal.

In order to determine the length of the active region, the following equations system has to be solved:

$$\begin{cases} k_0 \Delta n_{eff_{cross}} L = q\,\delta \\ k_0\, \Delta n_{eff_{bar}} L = (q+1)\delta \end{cases} \tag{6}$$

where $\Delta n_{eff_{cross}}$ and $\Delta n_{eff_{bar}}$ are the difference between the effective indices of the two propagating modes in the *cross* state and in the *bar* state, respectively; L is the length of the active region and q is an integer. The shortest value of L, solving the system (6), is:

$$L = \frac{1}{k_0} \frac{\delta}{\Delta n_{eff_{CROSS}} - \Delta n_{eff_{BAR}}} = \frac{1}{2} \frac{\ddot{e}}{\Delta n_{CROSS\text{-}BAR}} \tag{7}$$

where $k_0 = 2\pi/\lambda$ is the vacuum propagation vector, $\lambda = 1.55$ μm is the working wavelength and $\Delta n_{CROSS-BAR} = \Delta n_{eff_{CROSS}} - \Delta n_{eff_{BAR}}$

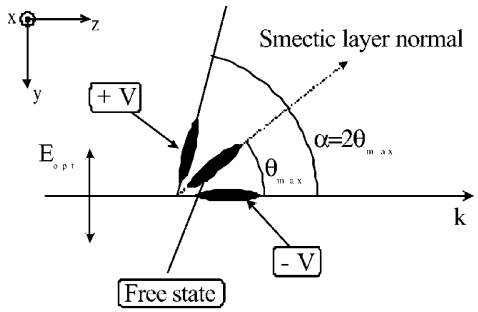

FIGURE 2 Operating principle of the LC/router.

For the configuration of our electro-optical router a planar alignment with the smectic normal layer tilted of an angle equal to θ_{max} with respect to z direction (free state in fig. 2) has been supposed. By applying an electric field, the LC molecules tilt in the plane of waveguide (the y-z plane as depicted in Fig.2) letting the angle between the average molecular optic axis and the incident beam direction θ to change. In such a way, being the molecules aligned parallel to the confining glass waveguide and referring to a TE mode as input field, the electro-optic effect turns into a modulation of the LC extraordinary refractive index and the output polarization is still linear.

The well-known extraordinary refractive index dependence on the angle ϑ between the optic axis and the incident beam direction is given by:

$$n_{LC}(\vartheta) = \frac{n_o\, n_e}{\sqrt{n_o^2 \sin^2(\vartheta) + n_e^2 \cos^2(\vartheta)}} \qquad (8)$$

where n_0 is the ordinary refractive index and n_e is the extraordinary one.
In particular, by applying the following voltage values: V_{max} and $-V_{max}$, tilt angle $+\theta_{max}$ and $-\theta_{ma}$ are achieved. As a consequence the following

values for the refractive index of the liquid crystal over-layer, according to eq. (8), are obtained : $n_{LC}(\vartheta=0)=n_o$ or $n_{LC}(\vartheta=2\cdot\theta_{max})$, depending on the device working condition (the *cross* and the *bar* state respectively).

Simulation results

In order to simulate the router working, a commercially available *smectic A** liquid crystal (BDH764E [from BDH catalog]) has been considered as cover of the active region. This liquid crystal presents, at wavelength λ=1.55 μm, an ordinary and an extraordinary refractive index equal to n_o=1.50 and n_e=1.65, respectively, and a maximum value of the tilt angle equal to θ_{max}=10° [22].

As evident from (7), in order to obtain a short optoelectronic device, a maximization of the difference $\Delta n_{CROSS-BAR}=\Delta n_{eff_{CROSS}}-\Delta n_{eff_{BAR}}$ has to be achieved. By means of SELENE software, simulations for the calculation of the two-dimensional field profile in cross-sections of the active region have been carried out. In the *cross* state, according to realized alignment, the supported modes of the active region (TE_{00} and TE_{01}) experience the ordinary refractive index of liquid crystal over-layer, so a $\Delta neff_{cross}=8.19\cdot10^{-3}$ has been obtained.

In order to determine the length L of the active region, the Δ_{neff} for the *bar* state relative to a tilt angle of $2\cdot\theta_{max}$ has to be evaluated. According to equation (8), the refractive index of the cover of active region is n_c=1.5154 at tilt angle of 20°. The consequent variation on the propagating characteristic of the active region involves a $\Delta n_{eff_{BAR}}=8.08\cdot10^{-3}$, which established a $\Delta n_{CROSS-BAR}\cong1.1\cdot10^{-4}$. Consequently, the length L needed to guarantee the additional π shift, in order to steer the light on the other side of the output Y-branch, is of about 7200 μm. In fig. 3 the spatially interference upon propagation in the active region is shown in both cross and bar states.

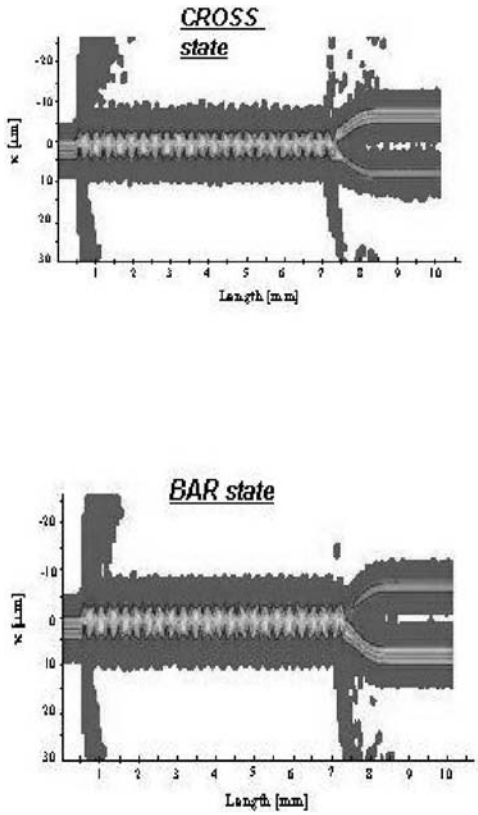

FIGURE 3 Beam propagation inside the device in *cross* and *bar* state.

In fig. 4, the field distribution presents on the two output waveguides is reported in both states [30]. For the proposed configuration an overall crosstalk (calculated as the average crosstalk between the cross and the bar state) of 6 dB is estimated. In order to increase the crosstalk an optimization both of the output Y-branch and of the coupling between the input waveguide and one bimodal, has to be sought. From fig.4 a good symmetric behavior of the router, when it switches between the *CROSS* and the *BAR* state, can be noted.

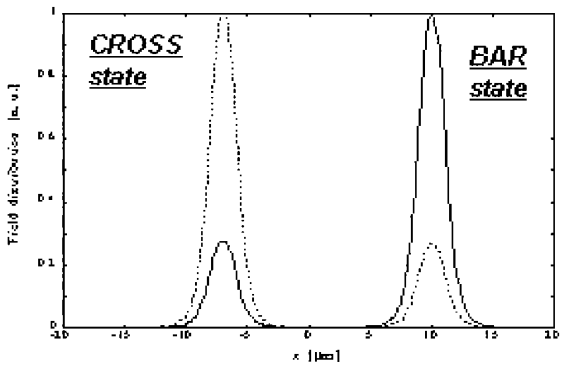

FIGURE 4 Field distribution on the output waveguides in cross state (dashed line) and in bar state (solid line).

CONCLUSIONS

In this paper, for the first time, we have proposed and analyzed an electro-optical router, based on self-imaging principle, in sol-gel channel waveguide with a liquid crystal overlayer. The electro-optic effect of smectic A* liquid crystals allows steering the spatially interfere between the two modes supported by the active region, leading to a localized output optical power maximum on one side (*bar state*) or the other (*cross state*) of the channel end-facet, depending on their relative phase. Numerical simulations have shown that the router exhibits satisfactory performances. The principal advantages of such device include fast tuning speed, low power consumption and low cost.

A further investigation is in progress in order to study the possibility of obtaining a tunable power splitting ratio utilizing the continuous effect of smectic A* liquid crystals.

Acknowledgements

Prof. G. Abbate from the "Dipartimento di Scienze Fisiche, Università di Napoli and Prof. G. C. Righini from IROE –CNR Firenze are gratefully acknowledged for very helpful discussions.

References

[1.] M. Bachmann, M. K. Smit, L. B. Soldano, P. A. Besse, E. Gini and H. Melchior, *Proc. Conf. Opt. Fiber Commun. (OFC)*, San Jose, CA, 32, (1993).

[2.] J. E. Zucker, K. L. Jones, T. H. Chiu and K. Brown-Goebeler, *J. Lightwave technology*, **10,** 12, 1926, (1992).

[3.] R. J. Deri, E. C. M. Penninngs, A. Scherer, A. S. Gozdz, C. Caneau, N. C. Andreadakis, V. Shah, L. Curtis, R. J. Hawkins, J. B. D. Soole and J. I. Song, *Photon. Technol. Lett.*, **4,** 11, 1238, (1992).

[4.] R. van Roijen, E. C. M. Pennings, M. J. N. van Stralen, J. M. M. van der Heijden, T. van Dongen, and B. H. Verbeek, *Appl. Phys. Lett.*, **64**, 14, 1753, (1994).

[5.] W. Y. Lee, J. S. Lin, K. Y. Lee, W. C. Chuang, *J. of Lightwave technology*, **13,** 11, 2236, (1995).

[6.] G. Scalia, D. Hermann, G. Abbate, L. Komitov, P. Mormile, G. C. Righini, L. Sirleto, *Mol. Cryst. Liq. Cryst.*, **320**, 321, (1998).

[7.] J. Patel, M. A. Saifi, C. Lin, *Appl. Phys. Lett.*, **57**, 1718, (1990).

[8.] D. Hermann, F. De Marco, G. Scalia, L. Sirleto, G. C. Righini, M. Lindgren, G. Abbate, *Mol. Cryst. Liq. Cryst.*, 352, 379, (2000).

[9.] Y. Uchiyama, M. Ozaki, K. Yoshino, *Ferroelectrics*, **149,** 217, (1993).

[10.] M. Ozaki, Y. Sadohara, T. Hatai and K. Yoshino, *Jpn. J. Appl. Phys.*, **29**, 843, (1990).

[11.] D.B. Walzer, E. N.Glytsis, T.K. Gaylord, *Applied Optics*, **35,** (16), 3016, (1996).

[12.] Y. Shani, C. Henry, R.C. Kistler, R.F. Kazarinov, K.J Orlowsky, *IEEE J. Quantum Electr.*, **27,** 31, 556, (1991).

[13.] S. Lindgren, M.G. Oberg, J. Andre, S. Nilsson, B. Broberg, B. Holmberg, L. Backbom, *J. Lightwave. Techn.*, **8,** 10, 1591, (1992).

[14.] R. M. de Ridder, A.F.M. Sander, A. Driessen, J.H.J. Fluitman, *J. Lightwave Techn.*, **11,** 1806, (1993).

[15.] C. C. Lee, T.J. Su, *Appl. Optics*, **33**, 7016, (1994).

[16.] N. A. Clark, S. T. Lagerwall, *Ferroelectric liquid crystals: principles, properties and applications*, Ed. J. Goodby Philadelfia, (1991).

[17.] G. Andersson, I. Dahl, L. Komitov, S. T. Largerwall, K. Sharp, B. Stebler, *J. Appl. Phys,* **66,** 4983, (1988).

[18.] G. Andersson, I. Dahl, W. Kuczynski, S. T. Largerwall, K. Sharp, B. Steble, *Ferroelectrics,* **84**, 285, (1998).
[19.] I. Abdulhalim, G. Moddel, *Liquid Crystal,* **9**, 493, (1991).
[20.] G. Andersson, I. Dahl, P. Keller, W. Kuczynski, S. T. Largerwall, K. Sharp, B. Stebler, *Appl. Phys.,* **51,** 9, 640, (1987).
[21.] Y. Bao, A. Sneh, K. Hsu, K. M. Johnson, J. Y. Liu, C. M. Miller, Y. Monta, M.B. McClain, *IEEE Photonics Technology Letters*, **8**, 1190, (1996).
[22.] A. Sneh, K. M. Johnson, J. Liu, *J. Lightwave. Techn*, **14,** 6, 1067, (1996).
[23.] R. Ulrich, *Optics Communications*, **13**, 3, 259, (1975).
[24.] R. Ulrich, G. Ankele, *Appl. Phys. Lett.*, **27**, 6, 253, (1975).
[25.] L.B. Soldano, E. C. M. Pennings, *J. Ligthwave. Tech.*, 13, 615, (1995)
[26.] L. B. Soldano, F. B. Veermann, M. K. Smit, B. H. Verbeek, A. H. Dubost, and E. C. M. Pennings, *J. Lightwave Technology*, **10**, 12, 1843, (1992).
[27.] P. A. Besse, M. Bachmann, H. Melchior, L. B. Soldano and M. K. Smit, *J. of Lightwave Technology*, **12,** 6, 1004, (1994).
[28.] S. Marteculli, A. N. Chester, M. Bertolotti, Eds *Advances in integrated optics*, New York: Plenum, (1994).
[29.] S. I. Najafi, T. Touam, R. Sara, M. P. Andrews, M. A. Fardad, *J Lightwave Tech*. **16,** 9, 1640, (1998).
[30.] BBV software. User's Manual: *Selene, Phrometius.*